Far East J. Appl. Math. **19**(3) (2005), 265-296

HEAT AND MASS TRANSFER OF MAGNETOHYDRODYNAMIC FLOW OF NON-NEWTONIAN FLUID THROUGH POROUS MEDIUM UNDERLYING AN AXISYMMETRIC SPREADING SURFACE

NABIL T. M. EL-DABE, MONA A. A. MOHAMED and M. A. HASSAN

Mathematics Department, Faculty of Education
Ain Shams University, Heliopolis, Cairo, Egypt

Abstract

In this paper we studied the effect of non-uniform permeability and magnetic field strength on heat and mass transfer for the flow of non-Newtonian fluid (biviscosity fluid) underlying an axisymmetric spreading surface. In modeling the flow, when the magnetic field strength and permeability are depending on the radial distance r, similarity solutions were utilized to represent the governing equations with appropriate boundary layer assumptions. The biviscosity model was used to characterize the non-Newtonian fluid behavior. Numerical results for the governing boundary layer equations were obtained by applying the quasi-linearization method. The results have been shown graphically, and the effect of non-dimensional parameters of the problem, such as, M (magnetic parameter), β (parameter denotes the upper limit of apparent viscosity), K_0 (permeability parameter), n (the surface temperature and concentration variation parameter), Sc (Schmidt number), Sr (Soret number), Df (Dufour number), and Pr (Prandtl number) illustrated on the velocity, temperature and

2000 Mathematics Subject Classification: 47.85.-9.

Key words and phrases: magnetohydrodynamic, non-Newtonian, biviscosity, heat transfer, mass transfer, porous medium.

Communicated by Belal Abdel-Aziz Dawoud

Received August 28, 2004; Revised February 7, 2005

concentration. Also, values of the skin friction C_f, Nusselt number Nu and Sherwood number Nm are tabled and illustrated by accompanying profiles.

Nomenclature

a, b Constants, defined in equation (9)

B Magnetic field strength [Wb/m^2]

C Concentration [–]

c_p Specific heat capacity [J/(kg.K)]

c_s Concentration susceptibility [J^{-1}.kg]

Df Dufour number [–]

D_m Mass diffusivity [m^2/s]

e_{ij} The deformation rate component [1/s]

F Constant = Q/2πh [m^2/s]

f Dimensionless stream function [–]

h Spreading film thickness [m]

h_w Rate of mass transfer, defined in equation (25)

K Permeability of the porous medium [m^2]

k_T Thermal diffusion ratio [–]

M Magnetic parameter [–]

n Parameter of surface temperature and concentration variation [–]

Nu Nusselt number [–]

Nm Sherwood number [–]

Pr Prandtl number [–]

p_y Yielding stress [Pa]

Q Volume flux at the surface $[m^3/s]$

q_w Rate of heat transfer, defined in equation (25)

r Radial coordinate [m]

Sc Schmidt number [–]

Sr Soret number [–]

T Temperature [K]

T_m Mean fluid temperature [K]

u Radial velocity component [m/s]

w Axial velocity component [m/s]

z Axial coordinate [m]

Greek symbols

μ Plastic viscosity of the fluid $[N.s/m^2]$

σ Electric conductivity [1/(ohm.m)] or $[\Omega^{-1}/m]$

ρ Density $[kg/m^3]$

α Thermal conductivity [W/(m.K)]

η Dimensionless coordinate [–]

τ_{ij} The shear stress components [Pa] or $[N/m^2]$

θ Temperature distribution function [–]

ϕ Concentration distribution function [–]

ν Kinematic viscosity of the fluid $= \mu/\rho$ $[m^2/s]$

$\pi_0 = e_{ij}e_{ji}$, where e_{ij} as defined above

β Dimensionless parameter denotes the upper limit of apparent viscosity coefficient, defined in equation (2)

Introduction

Industrial and biological flows through a spreading surface are quite common and have relevant applications such as, dip-coating of sheet metal, gravity drainage of paints, spin-coating of surface layers on silicon substrates, coating of inks on paper, spray-type heat exchangers, cooling towers, rotating condensers, evaporators and the study of spilling pollutant crude oil over the surface of sea water. One of the more important applications of the flow underlying an axisymmetric spreading surface is the spreading of blood through tissues and porous membranes in human body. On the other hand, many recent studies pointed out the importance of non-Newtonian characteristics of many fluids material, both in technology and in nature. A variety of non-Newtonian models have been developed in the last years, as an expression of the rheological properties of many fluids. Also, most of physiological fluids in the human body behave like non-Newtonian fluids. Blood is a suspension of red blood cells (erythrocytes), white blood cells (leukocytes) and platelets in a complex solution (called plasma) of gases, salts, proteins, carbohydrates, and lipids. Plasma is constituted by 90% water and can be considered as a Newtonian fluid. But, it is commonly assumed that blood is non-Newtonian fluid, because the elastic and deformable saturation of red cells gives it a shear dependent viscosity and a viscoelastic nature [3, 4, 11, 19, 24]. The viscosity, or internal friction, of blood increases as the percentage of cells in the blood increases, more cells mean more friction, which means a greater viscosity. The percentage of the blood volume occupied by red blood cells is called the *hematocrit*. Hematocrit is an important determinant of the viscosity of blood. As hematocrit increases there is an increase in viscosity, although the relationship is not linear (see Figure 1a). With a normal hematocrit of about 40 (that is, approximately 40% of the blood volume is red blood cells and the remainder plasma), the viscosity of whole blood (cells plus plasma) is about 3 times that of water (which is the reference viscosity). On the other hand, the viscosity of plasma alone is about 1.5 times that of water. Although the concentrations and types of proteins in the plasma can affect its viscosity, this has a little, if any, effect on the overall viscosity of whole blood. When the hematocrit rises to 60 or 70, which it often does in

patients with polycythemia, or abnormally high red blood cell counts, the blood viscosity can become as high as 10 times that of water. Alternatively, when the hematocrit falls drastically, as it does in patients with anemia (a decreased number of red cells in the blood), blood viscosity can approach that of plasma alone, therefore, a 50% increase in hematocrit from a normal value increases blood viscosity by about 100%. If we are interested in the raw numbers, the coefficient of viscosity for water is 0.001 Newton-second per meter squared (N.s/m^2 or Pa.s) at 20°C and the coefficient of viscosity for whole blood at the same temperature is 0.00345 Pa.s. Also, the coefficient of viscosity for whole blood at 37°C is 0.0027 Pa.s [12].

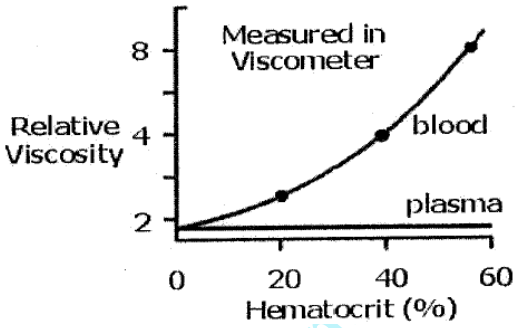

Figure 1a. Relative viscosity of all blood and plasma with hematocrit [17]

The relation between the viscosity of blood and hematocrit with the viscosity of plasma is $\mu_s = \mu_p(1 + 2.5H_t)$, considering μ_s = blood viscosity, μ_p = viscosity of plasma and H_t = hematocrit. But, the formula is not accurate for high values of hematocrit, for which the relation is no longer linear [29].

So, the blood is considered as a non-Newtonian fluid and in general Casson model is used as a constitutive equation of the blood, but, Nakamura and Sawada [21] have shown that there is no significant difference between Casson model and biviscosity model. Accordingly, the two constitutive equations resemble each other except in the very low shear rate region (see Figure 1b). In addition, the numerical calculations

based on the Casson model are very difficult to compare with the biviscosity model. Therefore, the biviscosity model can be used as a constitutive equation of blood and the calculated results are not affected very much [21]. Also, they have shown that the difference between the Casson model and the biviscosity model exists in a very low shear rate region and the calculated velocity distribution based on the biviscosity model agrees with that of measured by Casson model. So, in this study we can use the biviscosity model as a constitutive equation of blood.

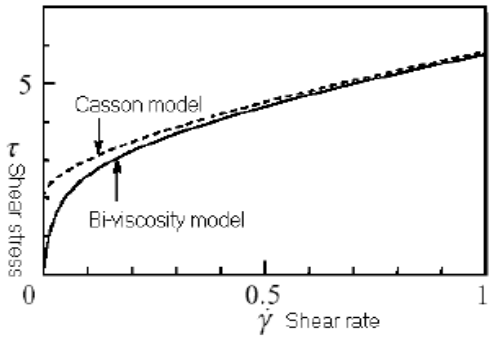

Figure 1b. Shear stress and shear rate correlation

The effect of axial magnetic field on the flow and heat transfer about a Newtonian fluid underlying an axisymmetric spreading surface is investigated by Lin and Chen [18]. Nakamura and Sawada [22] considered the starting and stopping flows of a biviscosity fluid through a pipe with and without stenosis. Also, many mathematical models for describing rheological behavior of blood have been extensively developed in the last decades [23, 27, 30, 31]. El-Dabe et al. [5-8] studied the MHD flow of non-Newtonian fluid through different flows, where the magnetic force is considered uniform during the motion. Also, El-Dabe et al. [9-10] studied the flow and heat transfer of MHD non-Newtonian Casson fluid between two rotating cylinders, and the flow of MHD non-Newtonian fluid with heat and mass transfer with heat source over an accelerating surface through a porous medium. Hong et al. [14] studied the effects of non-Darcian and non-uniform permeability conditions on the natural convection from a vertical plate in porous media. The effect of variable permeability of the porous medium for the natural convection

from inclined plate due to solar radiation was considered by Chamkha et al. [1]. Rahman et al. [25] studied the radially spreading flow of a thin liquid film with axisymmetric discharge of liquid through a thin slot and where a liquid jet impinges.

In this paper, we extend [18] to study the effect of an axial non-uniform magnetic field on the flow of non-Newtonian fluids. Especially, the effect of non-Newtonian property of blood on the flow with heat and mass transfer underlying an axisymmetric spreading surface through porous medium with non-uniform permeability using the biviscosity model as a constitutive equation of blood [16, 20].

Formulation of the Problem

We confined our attention on the most important biological fluid, the blood. While the linear theory of Navier-Stokes fluid is acceptable for modeling blood flow in large arteries, at shear rate higher than $100s^{-1}$, and when red blood cells not clump together therefore blood behaves as a Newtonian fluid. While, at low shear rate ($< 100s^{-1}$), red blood cells clump together to form aggregates and this behavior results for higher values of apparent viscosity. Then, the role of non-linearity and the effect of red cells on the viscosity become more important as well as in small vessels and for the spreading of blood through membranes [2]. Such flows cannot be well described by a simplistic linear constitutive equation. The biviscosity model [21] can be used as a constitutive equation of blood in some range of shear rates - as we illustrated above - where the shear stress can be written as

$$\tau_{ij} = \begin{cases} 2\left(\mu + \dfrac{p_y}{\sqrt{2\pi_0}}\right)e_{ij} & \pi_0 \geq \pi_c \\ 2\left(\mu + \dfrac{p_y}{\sqrt{2\pi_c}}\right)e_{ij} & \pi_0 < \pi_c \end{cases} \tag{1}$$

and

$$\beta = \frac{\mu\sqrt{2\pi_c}}{p_y}, \tag{2}$$

where β is a dimensionless parameter, which refers to the upper limit of

apparent viscosity coefficient. According to [21], when the mean shear rate of the calculation is about 20-150s^{-1}, the biviscosity model can be used as a constitutive equation instead of Casson model and calculated results are in a good agreement. Also it should be noted that, for the blood, the upper limit of apparent viscosity has a very large value and this means that β must take a small value.

The system under consideration is shown in Figure 2, it consists of a flow of an incompressible non-Newtonian fluid (blood) underlying a spreading film of thickness h lies in the plane $z = 0$, and the fluid is permeated by a non-uniform magnetic field with strength $B(r)$ in z-direction. Also, the fluid saturated porous medium (membrane) with non-uniform permeability $K(r)$ as a function of radial distance r. Transport through membrane takes place when a driving force is applied to the blood; these driving forces are a pressure difference ΔP, concentration difference ΔC, temperature difference ΔT or electric potential difference ΔE across the membrane [28]. In our study, we studied the concentration and temperature effects on the flow.

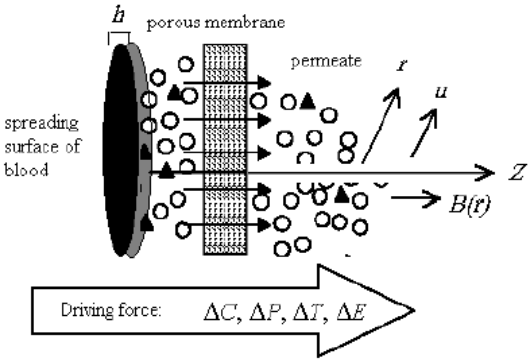

Figure 2. Schematic of spreading of blood through porous membrane with different driving forces that are present

Under these assumptions, and according to the boundary layer approximation with axisymmetric cylindrical polar coordinates (r, z), the steady laminar free convection flow of non-Newtonian fluid, is described by the following equations:

The continuity equation:

$$\frac{\partial(ru)}{\partial r} + \frac{\partial(rw)}{\partial z} = 0, \tag{3}$$

The equation of motion:

$$u\frac{\partial u}{\partial r} + w\frac{\partial u}{\partial z} = \frac{1}{\rho}\frac{\partial \tau_{rz}}{\partial z} - \frac{\sigma B^2(r)}{\rho}u - \frac{\mu}{\rho K(r)}u, \tag{4}$$

The energy equation:

$$\frac{\partial T}{\partial t} + w\frac{\partial T}{\partial z} = \frac{\alpha}{\rho c_p}\frac{\partial^2 T}{\partial z^2} + \frac{D_m k_T}{c_s c_p}\frac{\partial^2 C}{\partial z^2}, \tag{5}$$

The diffusion equation:

$$\frac{\partial C}{\partial t} + w\frac{\partial C}{\partial z} = D_m\frac{\partial^2 C}{\partial z^2} + \frac{D_m k_T}{T_m}\frac{\partial^2 T}{\partial z^2}, \tag{6}$$

where

$$\tau_{rz} = \left(\mu + \frac{p_y}{\sqrt{2\pi_c}}\right)\left(\frac{\partial u}{\partial z} + \frac{\partial w}{\partial r}\right). \tag{7}$$

The appropriate boundary conditions are

$$\left.\begin{array}{llllll} u = \dfrac{F}{r}, & w = 0, & T = T_w(r), & C = C_w(r) & z \to 0 \\ u = 0, & w = 0, & T = T_\infty, & C = C_\infty, & z \to \infty \end{array}\right\}, \tag{8}$$

where T_w, C_w and T_∞, C_∞ are the temperature and concentration at the surface and far away from it, respectively. We define $T_w(r) = T_\infty + ar^n$, $C_w(r) = C_\infty + br^n$, and the other symbols were listed in Nomenclature.

In order to simplify the governing equations (3)-(7) and the boundary conditions (8), we may introduce the following transformations:

$$\left.\begin{array}{ll} \eta = \sqrt{\dfrac{F}{\nu}}\dfrac{z}{r} & \psi = \sqrt{\nu F}\, rf(\eta) \\ u = \dfrac{1}{r}\dfrac{\partial \psi}{\partial Z} = \dfrac{F}{r}f' & w = -\dfrac{1}{r}\dfrac{\partial \psi}{\partial r} = -\dfrac{\sqrt{F\nu}}{r}(f - \eta f') \\ B(r) = \dfrac{B_0}{r} & K(r) = \dfrac{\nu r^2}{F}K_0 \\ T = T_\infty + ar^n\theta(\eta) & C = C_\infty + br^n\phi(\eta) \end{array}\right\}, \tag{9}$$

where n is the surface temperature and concentration variation parameter. Upon substituting the expression (9) into equations (3)-(7) and boundary conditions (8), one finds

$$\left(1+\frac{1}{\beta}\right)f''' + f'^2 + ff'' - \left(M+\frac{1}{K_0}\right)f' = 0, \tag{10}$$

$$\theta'' + Prf\theta' - nPr\theta f' + PrDf\phi'' = 0, \tag{11}$$

$$\phi'' + Scf\phi' - nSc\phi f' + ScSr\theta'' = 0, \tag{12}$$

with the boundary conditions

$$\left.\begin{array}{lllll} f=0 & f'=1 & \theta=1 & \phi=1 & \text{at} \quad \eta=0 \\ f'=0 & \theta=0 & \phi=0 & & \text{at} \quad \eta\to\infty \end{array}\right\}, \tag{13}$$

where the primes denote the partial differentiation with respect to the variable η. It should be noted that the dimensionless parameters are defined by

$M = \dfrac{\sigma B_0^2}{\rho F}$ Magnetic field parameter

$Pr = \dfrac{\mu c_p}{\alpha}$ Prandtl number

$Sc = \dfrac{\nu}{D_m}$ Schmidt number

$Df = \dfrac{D_m k_T (C_w - C_\infty)}{c_s c_p (T_w - T_\infty)\nu}$ Dufour number

$Sr = \dfrac{D_m k_T (T_w - T_\infty)}{T_m (C_w - C_\infty)\nu}$ Soret number.

Equations (10)-(12) with letting β, $K_0 \to \infty$, $Df = 0$ and ignoring equation (12) have been solved by Lin and Chen [18] for ordinary Newtonian fluid. The present problem treats a general case of non-Newtonian fluid to discuss the effect of rheological property of the fluid, which depends on β, and taking into account the flow through porous medium with considering the thermal diffusion and the diffusion-thermo effects on the flow.

Numerical Solution: Quasi-linearization Method

The set of equations (10)-(12) is highly non-linear ordinary differential equation, therefore this system of equations cannot be solved analytically. The quasi-linearization method has been used to transform these equations into a system of linear differential equations, and then we applied the method of complementary function to solving these yielding equations. The quasi-linearization method, which also known as the generalized Newtonian-Raphson method, was shown in details in [26]. This method is used due to following advantages:

1. The method is quadratically convergent, starting from the initial guess value.

2. The solution is valid for a large range of parameters. Even when the required number of initial conditions are not given, this method converges at a fast speed.

The quasi-linearization method applied for solving the equations (10)-(12) with rearrangement gives the following equations:

$$f''' = \frac{\beta}{1+\beta}\left(-f'^2 - ff'' + \left(M + \frac{1}{K_0}\right)f'\right), \tag{14}$$

$$\theta'' = \frac{1}{1 - PrDfScSr}\left(nPrf'\theta - Prf\theta' + ScDfPrf\phi' - nScDfPrf'\phi\right), \tag{15}$$

$$\phi'' = \frac{1}{1 - PrDfScSr}\left(nScf'\phi - Scf\phi' + ScPrSrf\theta' - nScPrSrf'\theta\right). \tag{16}$$

Define new variables as follows:

$$x_1 = f, \qquad x_2 = f', \qquad x_3 = f'',$$

$$x_4 = \theta, \qquad x_5 = \theta', \qquad x_6 = \phi,$$

$$x_7 = \phi'.$$

Using the above new variables, the system of higher order differential equations (14)-(16) and boundary conditions (13) may be transformed in to the another system of first order differential equations (17) and boundary conditions (18), respectively, as given hereunder

$$\left.\begin{aligned}
x_1' &= x_2 \\
x_2' &= x_3 \\
x_3' &= \frac{\beta}{1+\beta}\left(-x_2^2 - x_1 x_3 + \left(M + \frac{1}{K_0}\right)x_2\right) \\
x_4' &= x_5 \\
x_5' &= \frac{1}{1 - PrDfScSr}(nPrx_2x_4 - Prx_1x_5 + ScPrDfx_1x_7 - nScPrDfx_2x_6) \\
x_6' &= x_7 \\
x_7' &= \frac{1}{1 - PrDfScSr}(nScx_2x_6 - Scx_1x_7 + ScPrSrx_1x_5 - nScPrSrx_2x_4)
\end{aligned}\right\}, \tag{17}$$

$$\left.\begin{aligned}
\eta = 0 : \quad & x_1 = 0, \quad x_2 = 1, \quad x_4 = 1, \quad x_6 = 1 \\
\eta \to \infty : \quad & x_2 = 0, \quad x_4 = 0, \quad x_6 = 0
\end{aligned}\right\}. \tag{18}$$

Equations in (17) are in the form

$$x_i' = g_i(x_j, \eta) \quad (i, j = 1, 2, ..., m = 7), \tag{19}$$

where g_i's are taken as vectors in the mth dimensional space. The $(k+1)$th approximation $x_i^{(k+1)}$ to the solution of (19) is obtained by expanding the functional g_i about the kth approximation x_i^k, containing only the linear and constant terms. The kth approximation x_i^k is assumed to be a set of known approximate solutions.

By performing Taylor's series expansion of differential equations in (17), one can obtain the following equations expressed in matrix form:

$$\begin{pmatrix} x_1'^{(k+1)} \\ x_2'^{(k+1)} \\ . \\ . \\ . \\ x_7'^{(k+1)} \end{pmatrix} = \begin{pmatrix} a_{1,1} & a_{1,2} & \cdots & a_{1,7} \\ a_{2,1} & a_{2,2} & \cdots & a_{2,7} \\ . & . & & . \\ . & . & & . \\ . & . & & . \\ a_{7,1} & a_{7,2} & \cdots & a_{7,7} \end{pmatrix} \begin{pmatrix} x_1^{(k+1)} \\ x_2^{(k+1)} \\ . \\ . \\ . \\ x_7^{(k+1)} \end{pmatrix} + \begin{pmatrix} s_1 \\ s_2 \\ . \\ . \\ . \\ s_7 \end{pmatrix},$$

which can be written in the form

$$x_i'^{(k+1)} = a_{i,j} x_j^{(k+1)} + s_i, \qquad i, j = 1, 2, ..., 7 \tag{20}$$

or

$$X' = AX + S$$

with the boundary conditions

$$\left.\begin{array}{llll} x_1^{(k)}(0) = 0, & x_2^{(k)}(0) = 1, & x_4^{(k)}(0) = 1, & x_6^{(k)}(0) = 1, \\ x_2^{(k)}(\infty) = 0, & x_4^{(k)}(\infty) = 0, & x_6^{(k)}(\infty) = 0 & \end{array}\right\}. \tag{21}$$

The elements of the matrix $A_{7\times 7}$ and $S_{7\times 1}$ are thus obtained as given below

$$\left.\begin{array}{l} a_{ij} = \left(\dfrac{\partial g_i}{\partial x_j}\right)_{x^k} \\ s_i = g_i(x_j^k, \eta) - \displaystyle\sum_{j=1}^{m}\left(\frac{\partial g_i}{\partial x_j}\right)_{x^k} x_j^k \end{array}\right\} \text{ for } i, j = 1, 2, ..., m = 7. \tag{22}$$

The values of these elements $a_{i,j}$ and s_i are defined in the Appendix (part 1). The system given by equation (20) is linear in $x_i^{(k+1)}$ and its general solution can be obtained by using the method of complementary function, which determine the general solutions as particular and homogeneous solutions. The boundary conditions for the particular solution and homogeneous solution are given as follows:

(i) For the particular solution

$$q_i^{(k+1)}(0) = (0, 1, 0, 1, 0, 1, 0).$$

(ii) For the homogeneous solution

$$U_i^{(1)}(0) = (0, 0, 1, 0, 0, 0, 0),$$

$$U_i^{(2)}(0) = (0, 0, 0, 0, 1, 0, 0),$$

$$U_i^{(3)}(0) = (0, 0, 0, 0, 0, 0, 1).$$

Then, the general solution of the system of equation (20) is given by

$$x_i^{(k+1)}(\eta) = q_i^{(k+1)}(\eta) + \sum_{l=1}^{3} b_l U_i^{(l)}(\eta), \tag{23}$$

where b_1, b_2 and b_3 are the missing initial conditions and are determined by considering the boundary conditions at $\eta \to \infty$. The values of these constants defined in the Appendix (part 2).

The set of differential equations given in (20), have been solved by employing the fourth order Runge Kutta method for the boundary conditions given in (21) and solution is obtained by invoking the method of complementary function. The coefficients a_{ij} and s_i in (22) depend on the nominal trajectories $x_i^{(0)}(\eta)$. Hence, depending on the initial guess of nominal trajectories $x_i^{(0)}(\eta)$, the solution of equation (20) yields the neighboring trajectories $x_i^{(1)}(\eta)$. These neighboring trajectories are treated as nominal trajectories and the next neighboring trajectories are obtained, and this process is continued until the convergence is obtained. It is important to note that, the initial guess values for nominal trajectories need not be closer to the required solution. Any guess, such as, assuming zero values for all independent variables will be normally yield solutions. The whole range is divided into 100 equal parts with equal subinterval of width $\Delta\eta = 0.05$.

Results and Discussion

In the present analysis, we considered heat and mass transfer of non-Newtonian fluid (biviscosity fluid) through a porous medium underlying an axisymmetric spreading surface. After certain transformation, numerical solution has been obtained by quasi-linearization method. Then, the numerical results were obtained for distributions of velocity of spreading, temperature and concentration, according to different values of parameters of the problem; namely, the dimensionless parameter of upper limit of apparent viscosity β, magnetic parameter M, Schmidt number Sc, permeability parameter K_0, Soret number Sr, Dufour number Df and Prandtl number Pr.

One of the purposes of this study is to evaluate the effects of the non-Newtonian property of blood on its spreading through porous membranes in human body. The viscosity of blood effects its rate of flow through

small vessels and porous membranes. This phenomenon is illustrated in Figures 3-4. As seen from these figures the non-Newtonian property of blood (according to different values of β) works to decrease the functions f and f'. This implies that the velocity components u and w decrease as β increases. Therefore, the non-Newtonian property of blood can be one of the factors, which inhibit the spreading of blood through membranes. Also, in Figure 3 there is a comparison with Newtonian case, which is studied by [29], illustrated by dashing curve. Figure 5 shows that the absolute value of shear stress, according to different values of the function f'', decreases as β increases up to $\eta = 2$, but when $\eta > 2$ the inverse occur, and f'' asymptotically to zero when $\eta \to \infty$. Another resistance for the flow of blood is the magnetic parameter, as is shown from Figure 6 where the magnetic parameter reduces the flow velocity. It is expected that, an increase in the permeability of the porous membrane leads to a rise in the spreading of blood through it. This result is illustrated in Figure 7, where the velocity of the fluid increases as permeability parameter K_0 increases.

For blood, if the value of thermal conductivity $\alpha = 0.543\,\mathrm{W(m.K)}^{-1}$ and specific heat capacity $c_p = 4180\,\mathrm{J(kg.K)}^{-1}$, then the value of Prandtl number is about $Pr = 25$ for human blood [13], and for air at $20^{\circ}\mathrm{C}$ $Pr = 0.7$ [15]. We have seen from Figure 8 that the temperature decreases with increase in Prandtl number. Also, in the same figure the dependence of the blood viscosity on its temperature is illustrated, where a decrease in values of β corresponds to an increase in the temperature of blood for $n = 1$, while the inverse situation occurs at $n = -1$. The effect of permeability parameter K_0 on temperature and concentration distributions is plotted in Figures 9-10 for different values of n ($n = -1$, 0 and 1). The increase in the value of K_0 decreases the temperature and concentration distributions for $n = 0$ and -1, but for $n = 1$ the inverse occurs. In Figures 11-12 we illustrate the effect of the temperature difference $\Delta T = T_w - T_\infty$ and concentration difference $\Delta C = C_w - C_\infty$ on temperature and concentration profiles. In the case under

consideration, an increase in the values of Dufour number Df and a decrease in Soret number Sr means a decrease in the temperature difference ΔT, between the hot surface of spreading and the free stream, and an increase in the corresponding concentration difference ΔC. This leads to decreasing in the value of the dimensionless temperature $\theta(\eta)$ inside the thermal boundary layer (Figure 11), and this is clear for higher values of the dimensionless distance η from the hot surface. This result can be explained by the fact that the Dufour or diffusion-thermo effect becomes more important for smaller temperature differences and also for higher concentration differences. Inversely, it is evident from Figure 12 that when the concentration difference ΔC decreases and temperature difference ΔT increases (Sr increases or Df decreases) the dimensionless concentration profiles $\phi(\eta)$ decrease, in the sense that the value of ϕ decreases as the value of η increases. This result is a consequence of the increase of the thermal-diffusion parameter or Soret number. Figure 13 depicts the variation of dimensionless concentration function $\phi(\eta)$ with Schmidt number Sc for prescribed values of β. Profiles are shown both for $\beta = 0.005$ and $\beta = 0.01$. It is observed that the concentration is higher for $\beta = 0.005$ as compared to $\beta = 0.01$, i.e., the concentration is inversely proportional with β. Also, the concentration continuously decreases with an increase in Schmidt number. The variation in the temperature distribution with reference to the variation in magnetic parameter M for different values of Schmidt number Sc is presented in Figure 14. The results are given for negative value of n ($n = -1$). It is observed that the temperature values for $Sc = 0.2$ are more than that for $Sc = 0.5$. Also, from this figure we observed that as the magnetic parameter increases (i.e., an increase in the strength of applied magnetic field) the temperature continuously increases. The same pattern is observed for the concentration distribution in Figure 15. This indicates that the concentration can be increased by an increase in the magnetic field. While the concentration of the fluid reduces by increasing the value of Prandtl number, which corresponds to the fluid type; i.e., for blood $Pr = 25$ the concentration of the fluid is less than for air $Pr = 0.7$. The variation of

the dimensionless boundary layer thickness δ with β for different values of both M and K_0 is presented in Figures 16-17 and the accompanying Table 1. Here, δ is defined as the value of the similarity variable η at which the dimensionless velocity $f'(\eta)$ equals 0.01. It is observed from Figures 16-17 and Table 1 that the boundary layer thickness increases with permeability parameter K_0, and it can be reduced by increasing both β and M.

For the present problem, the local skin-friction can be written as

$$C_f = \sqrt{\frac{F}{\nu}} \frac{\tau_w}{\frac{1}{2}\rho\left(\frac{F}{r}\right)^2} = 2\left(1+\frac{1}{\beta}\right) f''(0), \tag{24}$$

where τ_w is the wall shear stress.

Obtaining temperature and concentration distributions, we can study the rate of heat and mass transfer. These rates can be written as

$$q_w = -\alpha\left[\frac{\partial T}{\partial z}\right]_{z=0}, \text{ and } h_w = -D_m\left[\frac{\partial C}{\partial z}\right]_{z=0}. \tag{25}$$

The local Nusselt number and the local Sherwood number Nu, Nm are defined by the following relations:

$$Nu = \frac{rq_w}{\alpha(T_w - T_\infty)}\sqrt{\frac{\nu}{F}} = -\theta'(0) \text{ and } Nm = \frac{rh_w}{D_m(C_w - C_\infty)}\sqrt{\frac{\nu}{F}} = -\phi'(0).$$

The numerical results for some values of $f''(0)$, $\theta'(0)$ and $\phi'(0)$ were obtained in Tables 2-4. Table 2 illustrates the variation of $f''(0)$ with the effective parameters of the velocity, which are M, K_0 and β. Since the shear stress $f''(0)$ represents the friction between the fluid flow and the surface, this friction increases as the fluid velocity increases and vice versa. Since the fluid velocity decreases as both M and β increase and increases as K_0 increases, the value of $f''(0)$ has the same behavior, i.e., reduces with an increase of M and β, and increases with an increase of K_0. The values of Nusselt and Sherwood numbers have been given for $n = -2$, $n = 1$ and $n = 2$ in Table 3 and for $n = 4$ in Table 4, which

show their variation with respect to all parameters of our problem. From the numerical results obtained as given in Table 3, it can be noticed that the rate of heat transfer and the rate of mass transfer have the same pattern, i.e., their values increase with an increase of M and β, while, these rates decrease with an increase in K_0. From Table 4 the rate of heat transfer has an opposite behavior compared to that of the rate of mass transfer, i.e., $\theta'(0)$ increases with Soret number Sr and decreases with the other parameters Schmidt number Sc, Prandtl number Pr and Dufour number Df, while $\phi'(0)$ has the inverse behavior.

Physical Applications

In this problem we studied the spreading of non-Newtonian fluid through a porous layer in the presence of variable magnetic field strength. An important type of non-Newtonian fluid is a viscoplastic or yield stress fluid. Bingham plastics are a special class of viscoplastic fluids that exhibit a linear behavior of shear stress against shear rate. An important example of these types of fluids is the blood. So, blood is considered to be a non-Newtonian fluid. The biviscosity model was used as a constitutive equation to describe the non-Newtonian property of blood. The applicable example for our problem is the flow of blood, which is considered as a non-Newtonian fluid, through porous membranes in human body. The spreading of blood through membrane takes place when a driving force is applied to it; we studied two types of these driving forces, which are concentration difference ΔC and temperature difference ΔT and its related parameters.

We mention here two applications corresponding to our results:

1. Very low flow states in the microcirculation occur during circulatory shock, the blood viscosity can increase quite significantly. This occurs because at low flow rates there are increased cell-to-cell and protein-to-cell adhesive interactions that can cause erythrocytes to adhere to one another and increase the blood viscosity [17]. This means that an increase in the blood viscosity leads to a decrease in its velocity of flow, this phenomenon is shown in Figure 3.

2. Temperature also has a significant effect on viscosity. As temperature decreases, viscosity increases (see Figure 8 for $n = 1$). Viscosity increases approximate 2% for each °C decrease in temperature. This effect has several implications. For example, when a person's hand is cooled upon exposure to a cold environment, the increase in blood viscosity contributes to the decrease in blood flow (along with neural-mediated thermoregulatory mechanisms). The use of whole body hypothermia during certain surgical procedures also increases blood viscosity and therefore increases resistance to blood flow [17].

Table 1. Numerical results for the dimensionless boundary layer thickness δ

β		K_0			M	
	0.2	0.5	0.8	10	15	20
0.01	9.3	9.45	9.5	9.5	9.2	8.85
0.02	8.05	8.6	8.75	8.65	7.75	6.9
0.03	6.9	7.65	7.85	7.75	6.55	5.75
0.04	6.1	6.9	7.15	7.00	5.75	5.00
0.05	5.55	6.35	6.6	6.45	5.2	4.5
0.06	5.15	5.95	6.25	6.1	4.8	4.15
0.07	4.8	5.65	6.00	5.8	4.5	3.85
0.08	4.55	5.4	5.75	5.55	4.25	3.65
0.09	4.35	5.25	5.6	5.4	4.05	3.45
0.1	4.2	5.1	5.5	5.25	3.9	3.3

Table 2. Numerical values of $f''(0)$ at $n = 4$, $Pr = 25$, $Df = 10$, $Sc = 20$, $Sr = 15$

β	K_0	M	$f''(0)$
0.01	0.2	5	– 0.31466963
0.02	0.2	5	– 0.44400287
0.03	0.2	5	– 0.54215267
0.01	0.2	5	– 0.31466963
0.01	0.2	10	– 0.38542688
0.01	0.2	15	– 0.44511524
0.01	0.2	10	– 0.38542688
0.01	0.5	10	– 0.34469549
0.01	0.8	10	– 0.33374573

Table 3. Numerical values of $\theta'(0)$ and $\phi'(0)$ for different values of n

	$\theta'(0)$			$\phi'(0)$		
	$n=-2$	$n=1$	$n=2$	$n=-2$	$n=1$	$n=2$
$\beta=0.005$	0.58991046	–0.17178066	–0.28642434	0.48016258	–0.15888259	–0.17842655
$\beta=0.01$	0.86215861	–0.15060519	–0.27996025	0.71911269	–0.14795133	–0.13991564
$\beta=0.02$	1.19592048	–0.12322711	–0.26977528	1.01233564	–0.13357643	–0.09074221
$M=5$	0.8608884	–0.15062428	–0.27992953	0.71828365	–0.14796479	–0.14002035
$M=10$	1.04975591	–0.13332377	–0.27135704	0.88460699	–0.13858672	–0.10971325
$M=20$	1.23230407	–0.11381816	–0.25863585	1.04591893	–0.12760955	–0.07656772
$K_0=0.1$	1.12219344	–0.12604851	–0.26705146	0.94852505	–0.13455057	–0.09720548
$K_0=0.4$	0.88549231	–0.14847085	–0.27897198	0.73993084	–0.14681191	–0.13621048
$K_0=0.7$	0.83605284	–0.15324288	–0.28105755	0.69164604	–0.14936193	–0.14466575

Table 4. Numerical values of $\theta'(0)$ and $\phi'(0)$ for different parameters of the problem

β	M	K_0	Sr	Sc	Pr	Df	$\theta'(0)$	$\phi'(0)$
0.01	5	0.2	15	20	25	10	– 0.14002524	– 0.63968175
0.02	5	0.2	15	20	25	10	– 0.10023263	– 0.57540332
0.03	5	0.2	15	20	25	10	– 0.07744655	– 0.53266295
0.01	5	0.2	10	20	5	10	– 0.36331682	– 0.46616821
0.01	10	0.2	10	20	5	10	– 0.33725361	– 0.43554638
0.01	15	0.2	10	20	5	10	– 0.31801400	– 0.41256149
0.01	10	0.2	15	25	20	10	– 0.12243221	– 0.60308489
0.01	10	0.5	15	25	20	10	– 0.13261217	– 0.62319120
0.01	10	0.8	15	25	20	10	– 0.13558458	– 0.62877579
0.01	5	0.2	10	20	25	10	– 0.42179256	– 0.41168107
0.01	5	0.2	15	20	25	10	– 0.14002524	– 0.63968175
0.01	5	0.2	20	20	25	10	– 0.10731087	– 0.64913957
0.01	5	0.2	10	5	25	15	– 0.63699862	– 0.14109781
0.01	5	0.2	10	10	25	15	– 0.63811786	– 0.14105136
0.01	5	0.2	10	20	25	15	– 0.63868444	– 0.14102256
0.01	10	0.2	10	20	0.7	10	– 0.25565150	– 0.49348682
0.01	10	0.2	10	20	5	10	– 0.33725361	– 0.43554638
0.01	10	0.2	10	20	25	10	– 0.39315013	– 0.38348246
0.01	10	0.2	15	20	20	10	– 0.12147827	– 0.60393707
0.01	10	0.2	15	20	20	15	– 0.29512038	– 0.29512038
0.01	10	0.2	15	20	20	20	– 0.34885959	– 0.19835983

References

[1] A. J. Chamkha, C. Issa and Khalil Khanafer, Int. J. Therm. Sci. 41 (2002), 73-81.

[2] S. Chien, S. Usami and R. Skalak, American Physiology Society Handbook of Physiology, Section 2, 4, pp. 217-249, 1984.

[3] H. Chmiel, I. Anadere and E. Walitza, Biorheology 27 (1990), 883-894.

[4] S. Deutsch, W. M. Phillips and J. Heist, Biorheology 13 (1976), 297-307.

[5] N. T. El-Dabe and M. O. El-Hassan, J. Ins. Math. Comp. Sci. 12 (1999), 249-261.

[6] N. T. El-Dabe and S. M. G. El-Mohandis, Arabian J. Sci. Engng. 20 (1986), 571-580.

[7] N. T. El-Dabe and S. M. G. El-Mohandis, J. Phys. Soc. Japan 64 (1995), 4165-4176.

[8] N. T. El-Dabe and El-Sakka, Acta. Physica Polonica A76 (1985), 823-828.

[9] N. T. El-Dabe and M. A. A. Mohamed, Chaos, Sol. Fractals 13 (2002), 907-917.

[10] N. T. El-Dabe, G. Saddeek and A. F. El-Sayed, Mech. Mech. Engng. Int. J. 5 (2001), 2.

[11] Y. C. Fung, Biodynamics: Circulation, Springer-Verlag, New York, 1984.

[12] A. C. Guyton and J. E. Hall, Textbook of Medical Physiology, 9th ed., Springer-Verlag, New York, 1996.

[13] D. Haemmerich, A. W. Wright, D. M. Mahvi, J. G. Webster and F. T. Lee, J. Med. Biol. Eng. Comput. 41 (2003), 317-323.

[14] J. T. Hong, Y. Yamada and C. L. Tien, J. Heat Transfer 109 (1987), 356-362.

[15] V. P. Isachenko, V. A. Osipova and A. S. Sukomel, Heat Transfer, Mir Publ., Moscow, 1977.

[16] M. Keentok, J. F. Milthorpe and E. O'donovan, J. Non-Newtonian Fluid Mech. 17 (1985), 23-25.

[17] Richard E. Klabunde, Cardiovascular Physiology Concepts, Internet site http://cvphysiology.com 1999-2003.

[18] C. R. Lin and C. K. Chen, J. Engng. Sci. 31(2) (1993), 257-261.

[19] D. E. Mann and J. M. Tarbell, Biorheology 27 (1990), 711-733.

[20] M. Nakamura and T. Sawada, J. Non-Newtonian Fluid Mech. 22 (1987), 191-206.

[21] M. Nakamura and T. Sawada, J. Biomech. Engng. 110 (1988), 137-143.

[22] M. Nakamura and T. Sawada, J. Biomech. Engng. 112 (1992), 100-103.

[23] C. Oiknine, Rheology of human blood, Adv. Cardiovasc. Phys. 5 (1983), 1-25.

[24] W. M. Phillips and S. Deutsch, Biorheology 12 (1975), 383-398.

[25] M. M. Rahman, A. Faghri and W. L. Hankey, Numerical Heat Transfer, Part A, 21 (1992), 101-120.

[26] S. M. Robert and J. S. Shipman, Two-point Boundary Value Problem Shooting Methods, American Elsevier Publ. Co., Inc., 1972.

[27] R. Skalak, N. Ozkaya and T. C. Skalak, Ann. Rev. Fluid Mech. 21 (1989), 167-204.

[28] M. Stanojevic, B. Lazarevic and B. Radic, FME Transactions 31 (2003), 91-98.

[29] Tables Scientifiques, Documenta GEIGY, settima edizione, CIBA-GEIGY S.A., Bale, 1973.

[30] G. B. Thurston, J. Biomech. 9 (1976), 13-20.

[31] F. J. Walburn and D. J. Schneck, Biorheology 13 (1976), 201-210.

Appendix

1. The elements of the matrix $A_{7\times7}$ and $S_{7\times1}$ are given as follows:

$$A = \begin{pmatrix} 0 & 1 & 0 & 0 & 0 & 0 & 0 \\ 0 & 0 & 1 & 0 & 0 & 0 & 0 \\ a_{3,1} & a_{3,2} & a_{3,3} & 0 & 0 & 0 & 0 \\ 0 & 0 & 0 & 0 & 1 & 0 & 0 \\ a_{5,1} & a_{5,2} & 0 & a_{5,4} & a_{5,5} & a_{5,6} & a_{5,7} \\ 0 & 0 & 0 & 0 & 0 & 0 & 1 \\ a_{7,1} & a_{7,2} & 0 & a_{7,4} & a_{7,5} & a_{7,6} & a_{7,7} \end{pmatrix} \text{ and } S = \begin{pmatrix} 0 \\ 0 \\ s_3 \\ 0 \\ s_5 \\ 0 \\ s_7 \end{pmatrix},$$

where the elements $a_{i,j}$ are defined as follows:

$$a_{3,1} = -\frac{\beta}{1+\beta} x_3^k, \qquad a_{3,2} = \frac{\beta}{1+\beta}\left(-2x_2^k + M + \frac{1}{K_0}\right),$$

$$a_{3,3} = -\frac{\beta}{1+\beta} x_1^k, \qquad a_{5,1} = \frac{1}{1 - ScSrDfPr}(ScDfPrx_7^k - Prx_5^k),$$

$$a_{5,2} = \frac{n}{1 - ScSrDfPr}(Prx_4^k - ScDfPrx_6^k),$$

$$a_{5,4} = \frac{nPr}{1 - ScSrDfPr} x_2^k,$$

$$a_{5,5} = \frac{-Pr}{1 - ScSrDfPr} x_1^k, \qquad a_{5,6} = \frac{-nScDfPr}{1 - ScSrDfPr} x_2^k,$$

$$a_{5,7} = \frac{ScDfPr}{1 - ScSrDfPr} x_1^k, \qquad a_{7,1} = \frac{1}{1 - ScSrDfPr}(ScSrPrx_5^k - Scx_7^k),$$

$$a_{7,2} = \frac{n}{1 - Sc\,Sr\,Df\,Pr}(Scx_6^k - Sc\,Sr\,Pr x_4^k),$$

$$a_{7,4} = \frac{-nSc\,Sr\,Pr}{1 - Sc\,Sr\,Df\,Pr}x_2^k,$$

$$a_{7,5} = \frac{Sc\,Sr\,Pr}{1 - Sc\,Sr\,Df\,Pr}x_1^k, \qquad a_{7,6} = \frac{nSc}{1 - Sc\,Sr\,Df\,Pr}x_2^k,$$

$$a_{7,7} = \frac{-Sc}{1 - Sc\,Sr\,Df\,Pr}x_1^k,$$

and the elements s_i are defined as follows:

$$s_3 = \frac{\beta}{1+\beta}(x_1^k x_3^k + x_2^k x_2^k),$$

$$s_5 = \frac{1}{1 - Sc\,Sr\,Df\,Pr}(Prx_1^k x_5^k - ScDf\,Prx_1^k x_7^k + nScDf\,Prx_2^k x_6^k - nPrx_2^k x_4^k),$$

$$s_7 = \frac{1}{1 - Sc\,Sr\,Df\,Pr}(Scx_1^k x_7^k - Sc\,Sr\,Pr x_1^k x_5^k + nSc\,Sr\,Prx_2^k x_4^k - nScx_2^k x_6^k).$$

2. The constants b_1, b_2, b_3 are given as follows:

$$b_1 = \frac{d_1}{d}, \qquad b_2 = \frac{d_2}{d}, \qquad b_3 = \frac{d_3}{d},$$

where

$$\begin{aligned} d &= U_2^{(1)}(\infty)(U_4^{(2)}(\infty)U_6^{(3)}(\infty) - U_4^{(3)}(\infty)U_6^{(2)}(\infty)) \\ &\quad - U_2^{(2)}(\infty)(U_4^{(1)}(\infty)U_6^{(3)}(\infty) - U_4^{(3)}(\infty)U_6^{(1)}(\infty)) \\ &\quad + U_2^{(3)}(\infty)(U_4^{(1)}(\infty)U_6^{(2)}(\infty) - U_4^{(2)}(\infty)U_6^{(1)}(\infty)), \\ d_1 &= q_2^{(k+1)}(\infty)(U_4^{(3)}(\infty)U_6^{(2)}(\infty) - U_4^{(2)}(\infty)U_6^{(3)}(\infty)) \\ &\quad + q_4^{(k+1)}(\infty)(U_2^{(2)}(\infty)U_6^{(3)}(\infty) - U_2^{(3)}(\infty)U_6^{(2)}(\infty)) \\ &\quad + q_6^{(k+1)}(\infty)(U_2^{(3)}(\infty)U_4^{(2)}(\infty) - U_2^{(2)}(\infty)U_4^{(3)}(\infty)), \end{aligned}$$

$$d_2 = q_2^{(k+1)}(\infty)(U_4^{(1)}(\infty)U_6^{(3)}(\infty) - U_4^{(3)}(\infty)U_6^{(1)}(\infty))$$
$$+ q_4^{(k+1)}(\infty)(U_2^{(3)}(\infty)U_6^{(1)}(\infty) - U_2^{(1)}(\infty)U_6^{(3)}(\infty))$$
$$+ q_6^{(k+1)}(\infty)(U_2^{(1)}(\infty)U_4^{(3)}(\infty) - U_2^{(3)}(\infty)U_4^{(1)}(\infty)),$$
$$d_3 = q_2^{(k+1)}(\infty)(U_4^{(2)}(\infty)U_6^{(1)}(\infty) - U_4^{(1)}(\infty)U_6^{(2)}(\infty))$$
$$+ q_4^{(k+1)}(\infty)(U_2^{(1)}(\infty)U_6^{(2)}(\infty) - U_2^{(2)}(\infty)U_6^{(1)}(\infty))$$
$$+ q_6^{(k+1)}(\infty)(U_2^{(2)}(\infty)U_4^{(1)}(\infty) - U_2^{(1)}(\infty)U_4^{(2)}(\infty)).$$

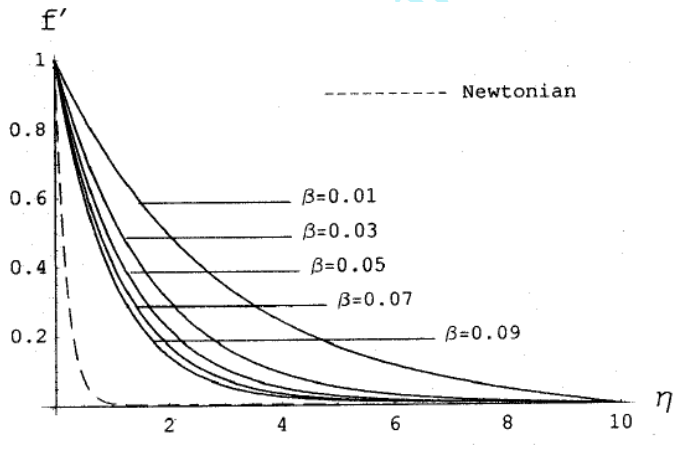

Figure 3. Velocity plotted versus position for different values of β at $Pr = 25$, $K_0 = 0.67$, $M = 10$, $Sc = 20$, $Df = 15$, $n = 3$, $Sr = 15$

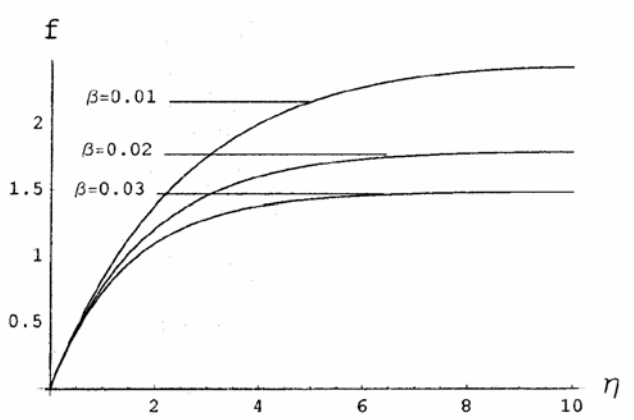

Figure 4. The similarity function f plotted versus position for the effect of β at $Pr = 25$, $K_0 = 0.2$, $M = 10$, $Sc = 20$, $Df = 5$, $Sr = 5$, $n = 4$

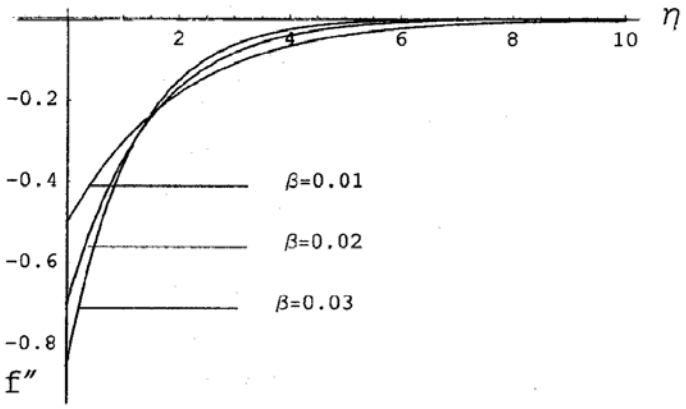

Figure 5. The similarity function f'' plotted versus position for the effect of β at $Pr = 25$, $K_0 = 0.2$, $M = 10$, $Sc = 20$, $Df = 5$, $Sr = 5$, $n = 4$

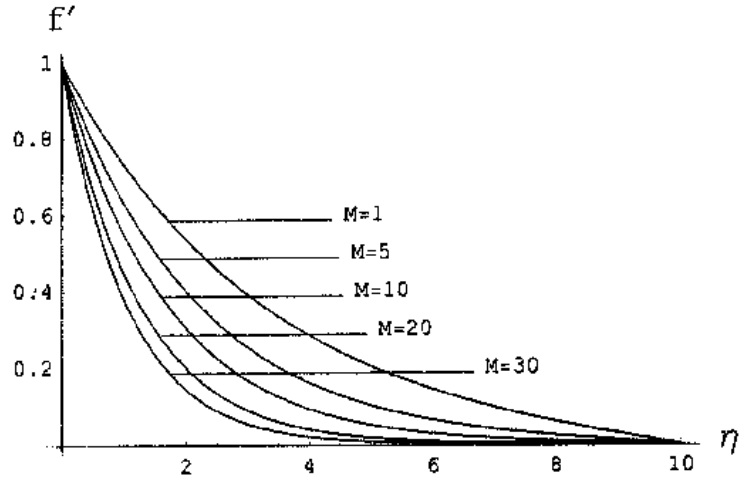

Figure 6. Velocity plotted versus position for the effect of magnetic parameter M at $Pr = 25$, $K_0 = 0.67$, $\beta = 0.03$, $Sc = 20$, $Df = 15$, $Sr = 15$, $n = 3$

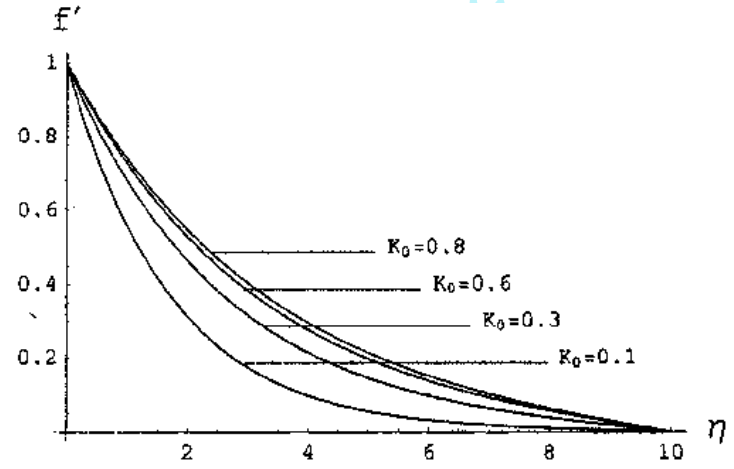

Figure 7. Velocity plotted versus position for the effect of permeability parameter K_0 at $Pr = 25$, $M = 1$, $\beta = 0.03$, $Sc = 20$, $Df = 15$, $Sr = 15$, $n = 3$

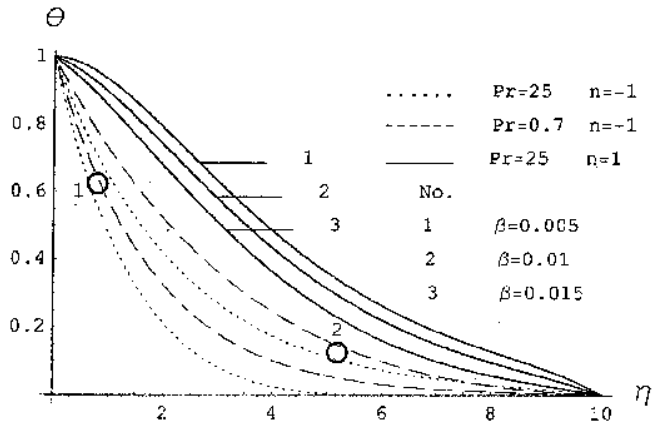

Figure 8. Temperature plotted versus position for the effect of Prandtl number Pr and different values of β at $K_0 = 0.5$, $M = 5$, $Sc = 0.5$, $Df = 6$, $Sr = 5$

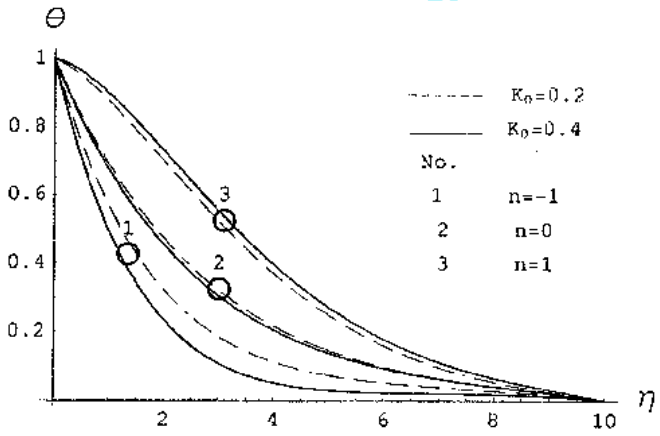

Figure 9. Temperature plotted versus position for the effect of temperature variation parameter n and permeability parameter K_0 at β = 0.01, $Pr = 25$, $M = 5$, $Sc = 10$, $Sr = 6$, $Df = 5$

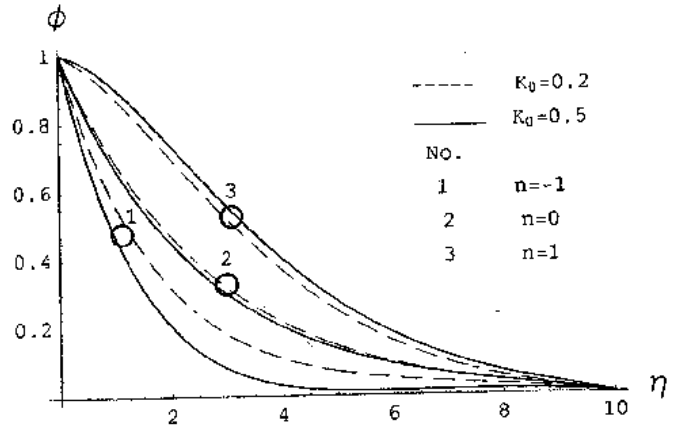

Figure 10. Concentration plotted versus position for the effect of concentration variation parameter n and permeability parameter K_0 at β = 0.01, Pr = 25, M = 5, Sc = 25, Sr = 5, Df = 6

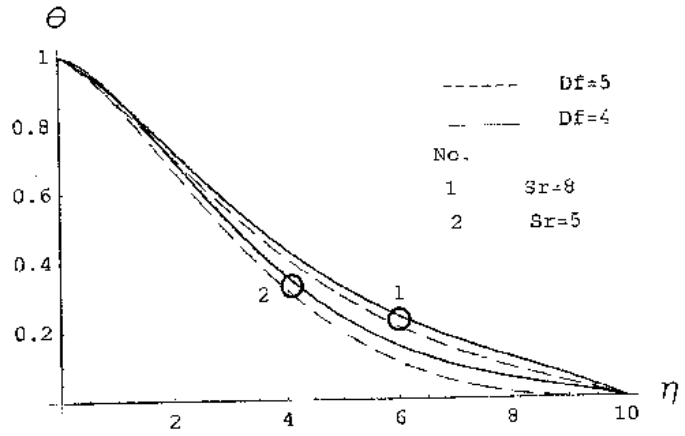

Figure 11. Temperature plotted versus position for the effect of Soret number Sr and Dufour number Df at β = 0.01, Pr = 25, M = 10, n = 1, Sc = 10, K_0 = 0.8

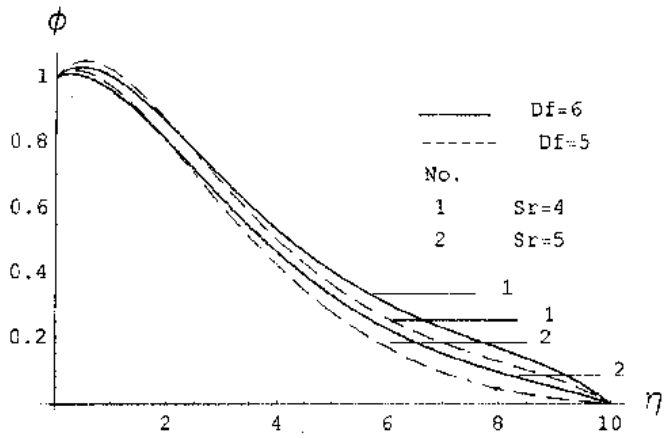

Figure 12. Concentration plotted versus position for the effect of Soret number Sr and Dufour number Df at $\beta = 0.003$, $Pr = 25$, $M = 10$, $Sc = 25$, $K_0 = 0.8$, $n = 1$

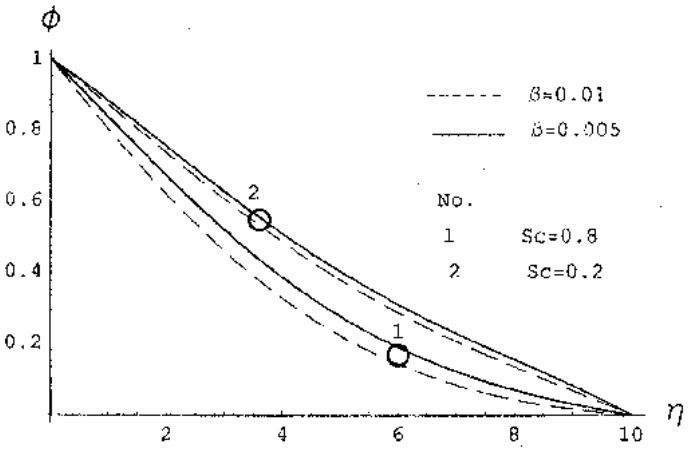

Figure 13. Concentration plotted versus position for the effect of Schmidt number Sc and different values of β at $K_0 = 0.7$, $M = 5$, $Pr = 25$, $Df = 20$, $Sr = 5$, $n = 1$

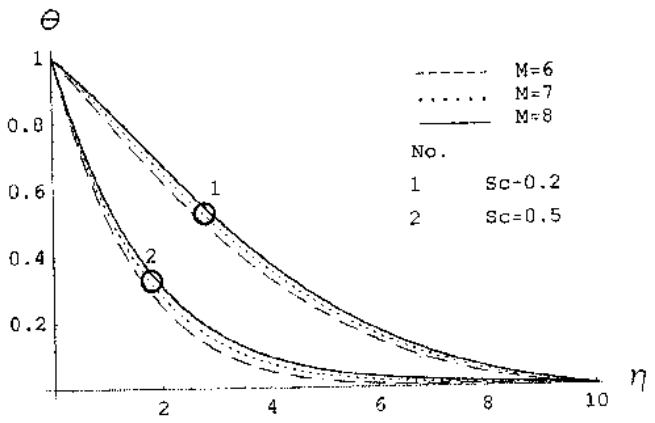

Figure 14. Temperature plotted versus position for the effect of magnetic parameter M and Schmidt number Sc at $\beta = 0.005$, $Pr = 25$, $n = -1$, $Sr = 5$, $K_0 = 0.5$, $Df = 6$

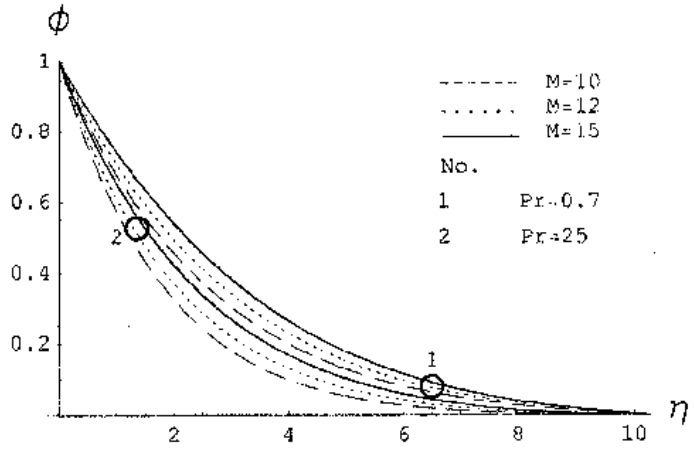

Figure 15. Concentration plotted versus position for the effect of magnetic parameter M and Prandtl number Pr at $\beta = 0.005$, $Df = 6$, $n = -1$, $Sc = 0.5$, $K_0 = 0.7$, $Sr = 5$

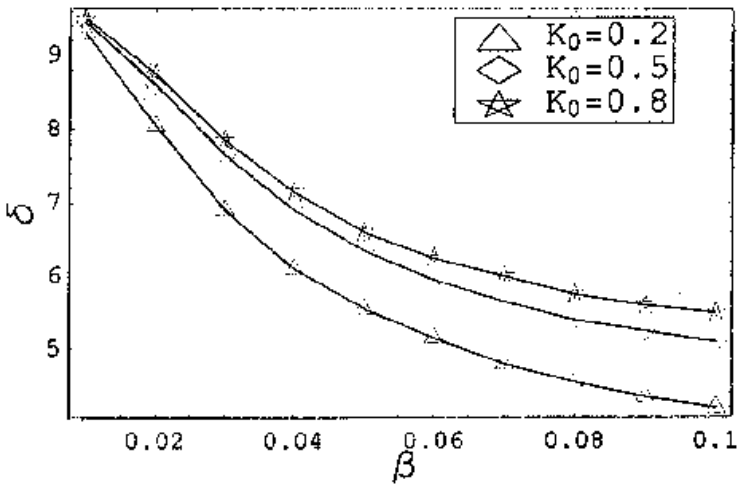

Figure 16. The boundary layer thickness plotted versus β for the effect of permeability parameter K_0 at $Pr = 20$, $M = 10$, $Sc = 20$, $Df = 20$, $n = 4$, $Sr = 15$

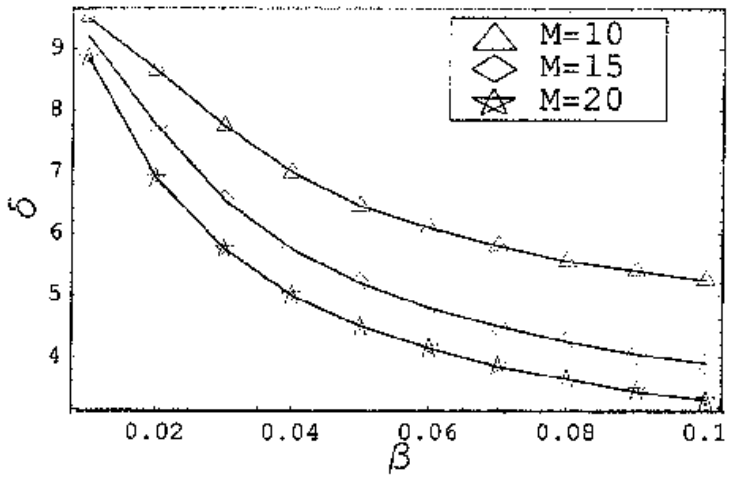

Figure 17. The boundary layer thickness plotted versus β for the effect of magnetic parameter M at $Pr = 20$, $K_0 = 0.6$, $Sc = 20$, $Df = 20$, $n = 4$, $Sr = 15$

■